A structure-preserving Partitioned Finite Element Method for the 2D wave equation

Flávio Luiz Cardoso-Ribeiro, Denis Matignon, Laurent Lefevre

A structure-preserving Partitioned Finite Element Method for the 2D wave equation ⋆

Flávio Luiz Cardoso-Ribeiro * **Denis Matignon** **
Laurent Lefèvre ***

* *Instituto Tecnológico de Aeronáutica, Brazil (e-mail:* flaviocr@ita.br*).*
** *ISAE-SUPAERO, Université de Toulouse, France (e-mail:* denis.matignon@isae-supaero.fr*).*
*** *Univ. Grenoble Alpes, LCIS, F-26902, Valence, France (e-mail:* laurent.lefevre@lcis.grenoble-inp.fr*)*

Abstract: Discretizing open systems of conservation laws while preserving the power-balance at the discrete level can be achieved using a new Partitioned Finite Element Method (PFEM), where an integration by parts is performed only on a subset of the variables in the weak formulation. Moreover, since boundary control and observation appear naturally in this formulation, the method is suitable both for simulation and control of infinite-dimensional port-Hamiltonian systems. The method can be applied using FEM software, and comes along with worked-out test cases on the 2D wave equation in different geometries and coordinate systems.

Keywords: Distributed Parameter systems, Port-Hamiltonian systems, Finite Element Method, Geometric Discretization Methods, 2D Wave equation.

1. INTRODUCTION

The port-Hamiltonian formalism has been proven to be a powerful tool for the modeling and control of complex multiphysics systems. In many cases, spatio-temporal dynamics must be considered and infinite-dimensional port-Hamiltonian models are needed. Classical academic examples such as the transmission line, the shallow water or the beam equations have been investigated in the port-Hamiltonian framework (Duindam et al., 2009). Besides, 2D and 3D problems have been recently considered (Wu et al., 2015; Vu et al., 2016; Trenchant et al., 2017). In many of these examples, systems of two balance equations are considered.

In order to simulate and design control laws, obtaining a finite-dimensional approximation which preserves the port-Hamiltonian structure of the original system can be advantageous. It may serve as a design guide such as in Control by Interconnection (CbI) or in Interconnection and Damping Assignment Passivity Based Control (IDA-PBC). Besides, preserving the underlying Dirac interconnection structure results in energy conservation properties and associated dynamical properties (e.g. stability, passivity, etc.).

In Golo et al. (2004), the authors proposed a mixed finite element structure-preserving spatial discretization for 1D hyperbolic systems of conservation laws, making use of the distinct low-order basis functions to approximate respectively the energy and co-energy variables. More recently, general geometric pseudo-spectral methods were proposed, using high-order global polynomial (Moulla et al. (2012)) or Bessel (Vu et al. (2017)) basis functions. An extension for the piezoelectric beam was proposed by Cardoso-Ribeiro et al. (2016). A finite volume structure-preserving discretization method was also investigated in Kotyczka (2016). Mixed finite element methods were also considered in Farle et al. (2014a, 2013, 2014b) where one of the equations is kept in strong form; numerical results were presented for one-dimensional systems only. A numerical study of a 2D vibro-acoustic system based on the mixed finite element method was performed by Wu et al. (2015). A 2D finite difference method with staggered grids was used to find a structure preserving scheme by Trenchant et al. (2017).

In these previous work, the central idea was to define different discretization spaces for the energy and co-energy variables such that the strong form of the equations was exactly satisfied in these finite-dimensional spaces. Defining these spaces is straightforward for 1D, but seems to be cumbersome for higher dimensions or higher order methods (Hiemstra et al., 2014). The kernel of the exterior derivatives in N-D dimensional domains is not anymore trivial and the discretization of the trace operator on boundaries with non trivial (i.e. rectangular) geometries often leads to dimensionality problems. As suggested in Kotyczka et al. (2018) the discretization of the weak formulation of the considered port-Hamiltonian system may be a practical solution to deal with these higher dimensional problems. We propose in this paper to follow this approach and to perform integration by parts on one of the two balance equations. Then, the discretization in the

⋆ This work is supported by the project ANR-16-CE92-0028, entitled *Interconnected Infinite-Dimensional systems for Heterogeneous Media*, INFIDHEM, financed by the French National Research Agency (ANR). Further information is available at https://websites.isae-supaero.fr/infidhem/the-project/.

chosen basis for the the energy and co-energy variables (and the associated test functions) leads directly to a full rank representation for the finite dimensional Dirac interconnection structure. Besides boundary conditions are naturally handled, even in the case of higher order finite element basis. Finally, differently from Farle et al. the use of weak-form in both equations enables to work with ready to use finite-element software to perform the proposed discretization scheme, and consequently to consider more involved problems and geometries. For instance, computations in the present paper have been done using the FreeFem++ software (Hecht, 2012).

This paper starts with the presentation of the wave equations in the partitioned weak form in Section 2. Secondly, we show that the discretized equations lead to a finite-dimensional port-Hamiltonian system in Section 3. Thirdly, the numerical scheme is applied to the simulation of the wave equation taking into account boundary excitation in Section 4. Finally in Section 5, we discuss how to make use of the method in other coordinate systems, and how to extend it to nonlinear (polynomial) systems, then some conclusions are drawn.

2. PARTITIONED WEAK FORM FOR THE WAVE EQUATION

In this section, we first recall how to write the strong form of the wave equation as a port-Hamiltonian system in § 2.1. Secondly, we propose a partitioned weak-form representation for this system in § 2.2, which will be discretized in the following section.

2.1 Wave equation as a system of conservation laws

The wave equation can be used to describe different phenomena like liquid sloshing, elasticity, propagation of electromagnetic waves in transmission lines, etc.

In vectorial form, the wave equation can be written as:

$$\begin{aligned} \dot{\alpha}_p(\boldsymbol{x},t) &= -\operatorname{div} \boldsymbol{e_q}(\boldsymbol{x},t)\,, \\ \dot{\boldsymbol{\alpha}}_q(\boldsymbol{x},t) &= -\boldsymbol{\nabla} e_p(\boldsymbol{x},t)\,, \end{aligned} \tag{1}$$

where $\boldsymbol{x} \in \Omega$ is the position vector, $\boldsymbol{e_q}$ and e_p are the co-energy variables, obtained from the variational derivatives of the system Hamiltonian with respect to the energy variables $\boldsymbol{\alpha}_q$ and α_p, respectively.

In the case of the linear wave equation, the Hamiltonian is given by:

$$H = \frac{1}{2}\int_\Omega \left(\alpha_p^2 + |\boldsymbol{\alpha}_q|^2\right) \mathrm{d}\Omega\,, \tag{2}$$

and the co-energy variables are computed as:

$$e_p = \frac{\delta H}{\delta \alpha_p} = \alpha_p\,, \quad \boldsymbol{e}_q = \frac{\delta H}{\delta \boldsymbol{\alpha}_q} = \boldsymbol{\alpha}_q\,. \tag{3}$$

The wave equation written as (1) is also known as a system of conservation laws. The spatial integral of the energy variables represent conserved quantities (e.g., total volume and linear momentum, in the shallow water equations, total charge and flux in the transmission line). Furthermore, the co-energy variables also exhibits physically relevant meaning (e.g., pressure and volumetric flow in the shallow water equations, voltage and current in the transmission line equations).

From the definition of the variational derivatives, The time-derivative of the Hamiltonian can be computed as:

$$\dot{H} = \int_\Omega \left(\dot{\boldsymbol{\alpha}}_q \cdot \frac{\delta H}{\delta \boldsymbol{\alpha}_q} + \dot{\alpha}_p \frac{\delta H}{\delta \alpha_p}\right) \mathrm{d}\Omega\,, \tag{4}$$

rewriting it in terms of the co-energy variables, we get:

$$\dot{H} = \int_\Omega \left(\dot{\boldsymbol{\alpha}}_q(\boldsymbol{x},t) \cdot \boldsymbol{e_q}(\boldsymbol{x},t) + \dot{\alpha}_p(\boldsymbol{x},t) e_p(\boldsymbol{x},t)\right) \mathrm{d}\Omega\,, \tag{5}$$

thus, from (1):

$$\begin{aligned} \dot{H} &= \int_\Omega \left(-\boldsymbol{\nabla} e_p(\boldsymbol{x},t) \cdot \boldsymbol{e_q}(\boldsymbol{x},t) - e_p(\boldsymbol{x},t) \operatorname{div} \boldsymbol{e_q}(\boldsymbol{x},t)\right) \mathrm{d}\Omega\,, \\ &= \int_{\partial\Omega} e_p(\boldsymbol{x},t) \left(-\boldsymbol{n} \cdot \boldsymbol{e_q}(\boldsymbol{x},t)\right)\, \mathrm{d}s\,, \end{aligned} \tag{6}$$

where the term $\boldsymbol{n}$ is the vector normal to the boundary curve $\partial\Omega$. Let us define the boundary input as:

$$u_\partial(s,t) := -\boldsymbol{n} \cdot \boldsymbol{e_q}(\boldsymbol{x}(s),t)) \quad s \in \partial\Omega\,. \tag{7}$$

Its power-conjugated boundary output is thus given by:

$$y_\partial(s,t) := e_p(\boldsymbol{x}(s),t) \quad s \in \partial\Omega\,, \tag{8}$$

and the power-balance reads:

$$\dot{H} = \int_{\partial\Omega} y_\partial(s,t) u_\partial(s,t)\, \mathrm{d}s\,. \tag{9}$$

2.2 Partitioned weak-form representation of the system of conservation laws

Instead of using vector variables in (1), let us rewrite the equations using its components: $\alpha_p(\boldsymbol{x},t) = \alpha_1(x,y,t)$, $\boldsymbol{\alpha}_q(\boldsymbol{x},t) = [\alpha_2(x,y,t)\ \alpha_3(x,y,t)]^T$. The equations become:

$$\begin{aligned} \dot{\alpha}_1(x,y,t) &= -\frac{\partial}{\partial x} e_2(x,y,t) - \frac{\partial}{\partial y} e_3(x,y,t) \\ \dot{\alpha}_2(x,y,t) &= -\frac{\partial}{\partial x} e_1(x,y,t) \\ \dot{\alpha}_3(x,y,t) &= -\frac{\partial}{\partial y} e_1(x,y,t) \end{aligned} \tag{10}$$

Let us take the arbitrary test functions $v_1(x,y)$, $v_2(x,y)$ and $v_3(x,y)$, and rewrite the previous equation using the following integral form:

$$\begin{aligned} \int_\Omega v_1 \dot{\alpha}_1 \,\mathrm{d}x\,\mathrm{d}y &= -\int_\Omega v_1 \left(e_{2,x} + e_{3,y}\right) \mathrm{d}x\,\mathrm{d}y\,, \\ \int_\Omega v_2 \dot{\alpha}_2 \,\mathrm{d}x\,\mathrm{d}y &= -\int_\Omega v_2 e_{1,x} \,\mathrm{d}x\,\mathrm{d}y\,, \\ \int_\Omega v_3 \dot{\alpha}_3 \,\mathrm{d}x\,\mathrm{d}y &= -\int_\Omega v_3 e_{1,y} \,\mathrm{d}x\,\mathrm{d}y \end{aligned} \tag{11}$$

integrating the first equation by parts, we get:

$$\begin{aligned} \int_\Omega v_1 \dot{\alpha}_1 \,\mathrm{d}x\,\mathrm{d}y &= \int_\Omega \left(v_{1,x} e_2 + v_{1,y} e_3\right) \mathrm{d}x\,\mathrm{d}y \\ &\quad - \int_{\partial\Omega} v_1 \boldsymbol{n} \cdot \begin{bmatrix} e_2(x,y,t) \\ e_3(x,y,t) \end{bmatrix} \mathrm{d}s\,, \\ \int_\Omega v_2 \dot{\alpha}_2 \,\mathrm{d}x\,\mathrm{d}y &= -\int_\Omega v_2 e_{1,x} \,\mathrm{d}x\,\mathrm{d}y\,, \\ \int_\Omega v_3 \dot{\alpha}_3 \,\mathrm{d}x\,\mathrm{d}y &= -\int_\Omega v_3 e_{1,y} \,\mathrm{d}x\,\mathrm{d}y\,. \end{aligned} \tag{12}$$

Note that the term $-\boldsymbol{n} \cdot \begin{bmatrix} e_2(x(s),y(s),t) \\ e_3(x(s),y(s),t) \end{bmatrix}$ is the boundary input, previously defined as $u_\partial(s,t)$ in (7).

From (12), we note that the variables of index 1 (v_1 and e_1) are derived once with respect to x and y, thus, they must be of class $H^1(\Omega)$. The variables of index 2 and 3 should be of class $L^2(\Omega)$ and should also have boundary values, thus belong to $H^{1/2}(\Omega)$.

In the following section, we discretize the partioned weak-form (12), and we show that the resulting system is a finite-dimensional port-Hamiltonian system and thus preserves the power-balance of the original system (9).

3. STRUCTURE PRESERVING FINITE ELEMENT DISCRETIZATION

Let us approximate the energy variables $\alpha_1(x,y,t)$ using the following basis with N_1 elements:

$$\begin{aligned}\alpha_1(x,y,t) \approx \alpha_1^{ap}(x,y,t) &:= \sum_{i=1}^{N_1} \phi_1^i(x,y)\alpha_1^i(t) \\ &= \boldsymbol{\phi}_1(x,y)^T \boldsymbol{\alpha}_1(t)\end{aligned} \tag{13}$$

The variables e_1 and v_1 are also approximated using $\boldsymbol{\phi}_1(x,y)$.

Similarly, the other energy variables are approximated as:

$$\begin{aligned}\alpha_2(x,y,t) \approx \alpha_2^{ap}(x,y,t) &:= \sum_{i=1}^{N_2} \phi_2^i(x,y)\alpha_2^i(t) \\ &= \boldsymbol{\phi}_2(x,y)^T \boldsymbol{\alpha}_2(t)\,,\end{aligned} \tag{14}$$

$$\begin{aligned}\alpha_3(x,y,t) \approx \alpha_3^{ap}(x,y,t) &:= \sum_{i=1}^{N_3} \phi_3^i(x,y)\alpha_3^i(t) \\ &= \boldsymbol{\phi}_3(x,y)^T \boldsymbol{\alpha}_3(t)\,.\end{aligned} \tag{15}$$

Furthermore, e_2 and v_2 are approximated using $\boldsymbol{\phi}_2(x,y)$, e_3 and v_3 are approximated using $\boldsymbol{\phi}_3(x,y)$.

Finally, the boundary input can be discretized using any one-dimensional set of basis functions, say $\boldsymbol{\psi} = [\psi^i]$:

$$u_\partial(s,t) \approx u_\partial^{ap}(s,t) := \sum_{i=1}^{N_\partial} \psi^i(s) u_\partial^i(t) = \boldsymbol{\psi}(s)^T \boldsymbol{u}_\partial(t)\,. \tag{16}$$

The finite-dimensional equations become:

$$\begin{aligned}\underbrace{\int_\Omega \boldsymbol{\phi}_1\boldsymbol{\phi}_1^T \,\mathrm{d}x\,\mathrm{d}y}_{M_1}\dot{\boldsymbol{\alpha}}_1 =& \underbrace{\int_\Omega \boldsymbol{\phi}_{1,x}\boldsymbol{\phi}_2^T \,\mathrm{d}x\,\mathrm{d}y}_{D_x}\boldsymbol{e}_2 \\ &+ \underbrace{\int_\Omega \boldsymbol{\phi}_{1,y}\boldsymbol{\phi}_3^T \,\mathrm{d}x\,\mathrm{d}y}_{D_y}\boldsymbol{e}_3 \\ &\underbrace{- \int_{\partial\Omega} \boldsymbol{\phi}_1(x(s),y(s))\Psi^T(s)\,\mathrm{d}s}_{B}\,\boldsymbol{u}_\partial(t)\,, \\ \underbrace{\int_\Omega \boldsymbol{\phi}_2\boldsymbol{\phi}_2^T \,\mathrm{d}x\,\mathrm{d}y}_{M_2}\dot{\boldsymbol{\alpha}}_2 =& -\underbrace{\int_\Omega \boldsymbol{\phi}_2\boldsymbol{\phi}_{1,x}^T \,\mathrm{d}x\,\mathrm{d}y}_{D_x^T}\boldsymbol{e}_1\,, \\ \underbrace{\int_\Omega \boldsymbol{\phi}_3\boldsymbol{\phi}_3^T \,\mathrm{d}x\,\mathrm{d}y}_{M_3}\dot{\boldsymbol{\alpha}}_3 =& -\underbrace{\int_\Omega \boldsymbol{\phi}_2\boldsymbol{\phi}_{1,x}^T \,\mathrm{d}x\,\mathrm{d}y}_{D_y^T}\boldsymbol{e}_1\,.\end{aligned} \tag{17}$$

The equations can be rewritten as:

$$\begin{aligned}M_1\dot{\boldsymbol{\alpha}}_1 =& D_x\boldsymbol{e}_2 + D_y\boldsymbol{e}_3 + B\boldsymbol{u}_\partial(t)\,, \\ M_2\dot{\boldsymbol{\alpha}}_2 =& -D_x^T\boldsymbol{e}_1\,, \\ M_3\dot{\boldsymbol{\alpha}}_3 =& -D_y^T\boldsymbol{e}_1\,,\end{aligned} \tag{18}$$

where M_1, M_2 and M_3 are square matrices (of size $N_1\times N_1$, $N_2\times N_2$ and $N_3\times N_3$, respectively). D_x is an $N_1\times N_2$ matrix, D_y is an $N_1\times N_3$ matrix and B is an $N_1\times N_\partial$ matrix.

The time derivative of the continous Hamiltonian (5) can be rewritten using the coordinate variables as:

$$\dot{H} = \int_\Omega (\dot{\alpha}_1 e_1 + \dot{\alpha}_2 e_2 + \dot{\alpha}_3 e_3)\,\mathrm{d}x\,\mathrm{d}y\,. \tag{19}$$

Using the approximated variables:

$$\dot{H} \approx \dot{\boldsymbol{\alpha}}_1^T M_1 \boldsymbol{e}_1 + \dot{\boldsymbol{\alpha}}_2^T M_2 \boldsymbol{e}_2 + \dot{\boldsymbol{\alpha}}_3^T M_3 \boldsymbol{e}_3\,, \tag{20}$$

Let us define new energy variables as:

$$\tilde{\boldsymbol{\alpha}}_1 := M_1\boldsymbol{\alpha}_1\,, \quad \tilde{\boldsymbol{\alpha}}_2 := M_2\boldsymbol{\alpha}_2\,, \quad \tilde{\boldsymbol{\alpha}}_3 := M_3\boldsymbol{\alpha}_3\,, \tag{21}$$

such that (20) becomes:

$$\dot{H} \approx \dot{\tilde{\boldsymbol{\alpha}}}_1^T \boldsymbol{e}_1 + \dot{\tilde{\boldsymbol{\alpha}}}_2^T \boldsymbol{e}_2 + \dot{\tilde{\boldsymbol{\alpha}}}_3^T \boldsymbol{e}_3\,, \tag{22}$$

We define the discretized Hamiltonian as:

$$\begin{aligned}H_d(\tilde{\boldsymbol{\alpha}}_1,\tilde{\boldsymbol{\alpha}}_2,\tilde{\boldsymbol{\alpha}}_3) := H\Big[&\alpha_1(\boldsymbol{x},t) = \left(M_1^{-1}\tilde{\boldsymbol{\alpha}}_1(t)\right)^T \boldsymbol{\phi_1}(\boldsymbol{x})\,, \\ &\alpha_2(\boldsymbol{x},t) = \left(M_2^{-1}\tilde{\boldsymbol{\alpha}}_2(t)\right)^T \boldsymbol{\phi_2}(\boldsymbol{x})\,, \\ &\alpha_3(\boldsymbol{x},t) = \left(M_3^{-1}\tilde{\boldsymbol{\alpha}}_3(t)\right)^T \boldsymbol{\phi_3}(\boldsymbol{x})\Big]\,.\end{aligned} \tag{23}$$

The time-derivative of this discretized Hamiltonian is given by:

$$\dot{H}_d = \dot{\tilde{\boldsymbol{\alpha}}}_1^T \frac{\partial H_d}{\partial \tilde{\boldsymbol{\alpha}}_1} + \dot{\tilde{\boldsymbol{\alpha}}}_2^T \frac{\partial H_d}{\partial \tilde{\boldsymbol{\alpha}}_2} + \dot{\tilde{\boldsymbol{\alpha}}}_3^T \frac{\partial H_d}{\partial \tilde{\boldsymbol{\alpha}}_3}\,. \tag{24}$$

Since we want that both power balances (20) and (24) coincide, the following constitutive relations must hold:

$$\boldsymbol{e}_1 = \frac{\partial H_d}{\partial \tilde{\boldsymbol{\alpha}}_1}\,, \boldsymbol{e}_2 = \frac{\partial H_d}{\partial \tilde{\boldsymbol{\alpha}}_2}\,, \boldsymbol{e}_3 = \frac{\partial H_d}{\partial \tilde{\boldsymbol{\alpha}}_3}\,. \tag{25}$$

Rewriting the finite-dimensional equations (18), we get the following finite-dimensional port-Hamiltonian system:

$$\begin{aligned}\begin{bmatrix}\dot{\tilde{\boldsymbol{\alpha}}}_1 \\ \dot{\tilde{\boldsymbol{\alpha}}}_2 \\ \dot{\tilde{\boldsymbol{\alpha}}}_3\end{bmatrix} =& \begin{bmatrix}0 & D_x & D_y \\ -D_x^T & 0 & 0 \\ -D_y^T & 0 & 0\end{bmatrix}\begin{bmatrix}\boldsymbol{e}_1 \\ \boldsymbol{e}_2 \\ \boldsymbol{e}_3\end{bmatrix} + \begin{bmatrix}B \\ 0 \\ 0\end{bmatrix}\boldsymbol{u}_\partial\,, \\ \boldsymbol{y}_\partial =& B^T\boldsymbol{e}_1\,,\end{aligned} \tag{26}$$

where $\boldsymbol{y}_\partial$ is the conjugated output of the discretized system.

From (24) and (26), the time derivative of the discretized Hamiltonian is given by:

$$\begin{aligned}\dot{H}_d &= \dot{\tilde{\boldsymbol{\alpha}}}_1^T\,\boldsymbol{e}_1 + \dot{\tilde{\boldsymbol{\alpha}}}_2^T\,\boldsymbol{e}_2 + \dot{\tilde{\boldsymbol{\alpha}}}_3^T\,\boldsymbol{e}_3\,, \\ &= \left(\boldsymbol{e}_2^T D_x^T + \boldsymbol{e}_3^T D_y^T + \boldsymbol{u}_\partial^T B\right)\boldsymbol{e}_1 - \boldsymbol{e}_1^T D_x\,\boldsymbol{e}_2 - \boldsymbol{e}_2^T D_y\,\boldsymbol{e}_3\,, \\ &= \boldsymbol{y}_\partial^T\,\boldsymbol{u}_\partial\,.\end{aligned} \tag{27}$$

Note that $\boldsymbol{u}_\partial^T\boldsymbol{y}_\partial$ is the discrete analog of the continuous power-balance equation (9). Furthermore, this power-balance is exactly preserved in the finite dimensional approximation spaces. From the definition of the B matrix (17), the definition of the approximated boundary

input $u_\partial^{ap}(s,t) := \boldsymbol{\psi}(s)^T \boldsymbol{u}_\partial(t)$ and approximated co-energy variable $e_1^{ap}(x(s),y(s),t) := \boldsymbol{\phi}_1(x(s),y(s))^T \boldsymbol{e}_1(t)$, we get:

$$\begin{aligned} \dot{H}_d &= \boldsymbol{e}_1^T \int_{\partial\Omega} \boldsymbol{\phi}_1(x(s),y(s)) \Psi^T(s)\,\mathrm{d}s\,\boldsymbol{u}_\partial\,, \\ &= \int_{\partial\Omega} e_1^{ap}(x(s),y(s),t) u_\partial^{ap}(s,t)\,\mathrm{d}s\,. \end{aligned} \tag{28}$$

Remark 1. Note that using classical finite-elements 1D discretization basis for the boundary input, $\boldsymbol{u}_\partial(s,t)$ provides the values of the influx $(-\boldsymbol{n}\cdot\boldsymbol{e_q})$ at the boundary nodes. For instance, in the case of shallow water equations, these are the values of volumetric influx into the system. The conjugated output $\boldsymbol{y}_\partial$ is related with the curve integral of $e_1(x(s),y(s),t)$ along the elements. The co-energy variable $e_1(x(s),y(s),t)$ is the pressure, thus the discretized outputs $\boldsymbol{y}_\partial$ are related to the forces per unit length applied along the external boundary.

Remark 2. With this choice of partition of variables, other boundary inputs and outputs can easily be dealt with: it is enough to define $\tilde{\boldsymbol{u}}_\partial := \Sigma\,\boldsymbol{u}_\partial$, and $\tilde{\boldsymbol{y}}_\partial := \Sigma\,\boldsymbol{y}_\partial$ for some orthogonal matrix Σ of dimension $N_\partial \times N_\partial$. Indeed, the power balance (27) is preserved thanks to orthogonality, and in (26), B is replaced by $B\,\Sigma^T$ for the control, and B^T is replaced by $\Sigma\,B^T$ for the collocated observation.

Remark 3. Different choices of variables are also possible for the integration by parts. Instead of integrating the first equation by parts in (12), we could integrate the two other equations, which would also lead to another skew-symmetric structure; the boundary inputs and outputs would not be the same either.

Remark 4. In the sequel, in our finite element method, we conveniently chose $\boldsymbol{\psi}(s)$ as $\boldsymbol{\phi}_1(x(s),y(s))$ evaluated at the boundary. Other choices could be investigated.

4. NUMERICAL EXPERIMENTS

In this section, several numerical experiments are presented with the goal of testing the proposed discretization scheme. Firstly, a numerical convergence analysis is presented in § 4.1. Different polynomial degrees for the discretized variables and number of elements were considered. Secondly, in § 4.2 the scheme is proven useful for simulating the system subjected to external boundary excitation. Finally, in § 4.3 we discuss one of the main advantages of this method (in comparison to other port-Hamiltonian discretization methods): it can be directly applied using available open source finite element software.

4.1 Convergence analysis

The power-preserving discretization method presented in the previous section was implemented using quadrilateral elements with polynomial basis functions for a square domain. The following Hamiltonian was considered:

$$H = \frac{1}{2}\int_\Omega \left(\alpha_1^2 + \alpha_2^2 + \alpha_3^2\right)\mathrm{d}\Omega\,, \tag{29}$$

where $\Omega = [0,1]\times[0,1]$. After discretization, using (23), the Hamiltonian reads:

$$H_d = \frac{1}{2}\left(\tilde{\boldsymbol{\alpha}}_1^T\, M_1^{-1}\tilde{\boldsymbol{\alpha}}_1 + \tilde{\boldsymbol{\alpha}}_2^T\, M_2^{-1}\tilde{\boldsymbol{\alpha}}_2 + \tilde{\boldsymbol{\alpha}}_3^T\, M_3^{-1}\tilde{\boldsymbol{\alpha}}_3\right)\,, \tag{30}$$

A convergence analysis of the numerical method was done, focusing on the spectrum of the discretized system. The eigenvalues obtained from the numerical model were compared to the exact eigenfrequencies of the linear wave equation with constant coefficients. The inputs of (26) (given by the influx through the boundaries) were considered to be zero, i.e.:

$$u_\partial(x,y,t) = 0\ ,[x,y]\in\partial\Omega\,, \tag{31}$$

or, in the finite-dimensional case, simply $\boldsymbol{u}_\partial = 0$.

Recall that the variables with index 1 (α_1, e_1, v_1) must be discretized with polynomials of order at least one (since they are derived once in (12)). Fig. 1 shows the relative error of the first modal frequency for three different choices of polynomial approximations. $P_1P_0P_0$ stands for first order polynomial for the variable 1, and order zero for the other two variables. $P_1P_1P_1$ uses first-order polynomial for the three variables. Finally, $P_1P_2P_2$ uses first-order polynomial for the first variable, and order two for the other two variables.

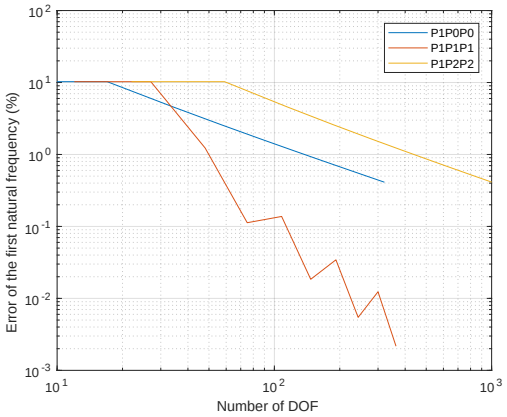

Fig. 1. Convergence of the first natural frequency of the 2D wave equation.

Remark 5. A more logical test case would be to use $P_2P_1P_1$ polynomials (instead of $P_1P_2P_2$, since the differentiability requirement is higher on the first variable). However, such a choice surprisingly did not lead to a convergent numerical scheme. It is also somewhat surprising that using $P_1P_1P_1$ leads to the best convergence rate among the three test cases (instead of the higher-order choice $P_1P_2P_2$). The convergence of the proposed scheme should be better investigated in further work.

4.2 Time domain simulations

Numerical time-domain simulations were performed using the discretized system under boundary-port excitation. The following boundary conditions were used:

$$u_\partial(x,y,t) = \begin{cases} \sin(\pi t)\ ,[x,y]\in\partial\Omega_{up}\,, \\ -\sin(\pi t)\ ,[x,y]\in\partial\Omega_{left}\,, \\ 0\ ,[x,y]\in\partial\Omega_{down}\cup\partial\Omega_{right}\,. \end{cases} \quad t\le 1s, \tag{32}$$

and $u_\partial(x,y,t) = 0, [x,y]\in\partial\Omega, t > 1s$. The boundary is split in four sides: $\partial\Omega = \partial\Omega_{up}\cup\partial\Omega_{left}\cup\partial\Omega_{down}\cup\partial\Omega_{right}$. These conditions impose a harmonic influx on one side of the boundary and the opposite condition at another side. Snapshots of this simulation are presented in Fig. 2. The simulations were performed using `lsim`, the MATLAB tool for linear systems simulation.

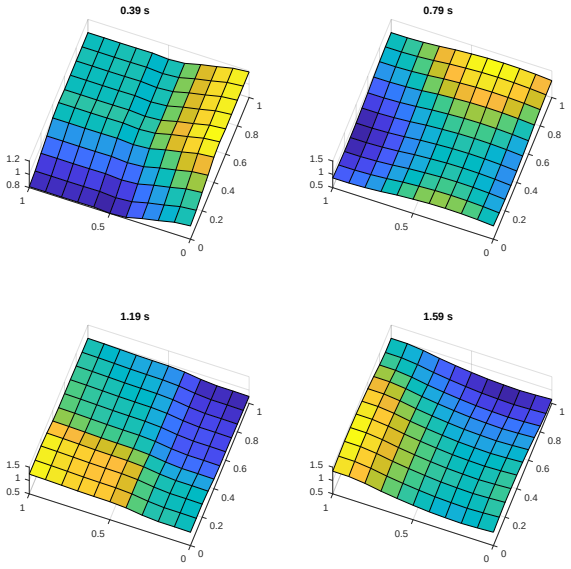

Fig. 2. Snapshots of simulation for a harmonic excitation at two of the boundaries of the domain. The variable α_1 is shown.

Finally, the convergence of the time domain simulation with boundary conditions given by (32) was verified. Fig. 3 shows the L_2 norm of the error, taking into account the state of the system after one second of simulation. The numerical result obtained using 1600 elements was taken as reference to compute the error. First-order convergence is observed for a choice of $P_1P_0P_0$ polynomials.

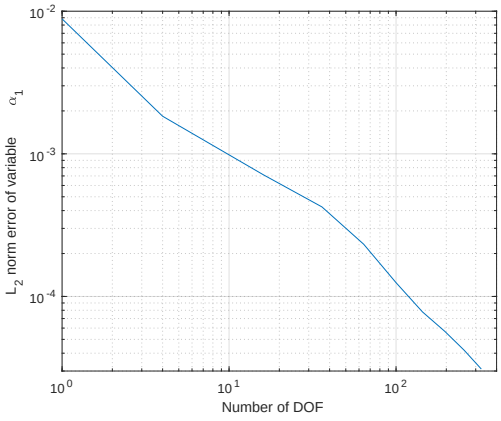

Fig. 3. Convergence of the L_2 error as a function of the number of degrees of freedom of the discretization scheme. The error is computed after 1 second of simulation. Polynomials of order 1, 0 and 0 were used as approximation functions for the variables ($P_1P_0P_0$). A first-order convergence is observed.

4.3 Using FEM software for more complex geometries

One of the main advantages of the method proposed in this paper compared to previous work on power-preserving discretization methods is that it proves compatible with classic FEM software.

For instance, the 2D mesh presented in Fig. 4 is quickly done using FreeFem++ (Hecht, 2012), and obtaining the matrices of (26) only requires a few lines of code.

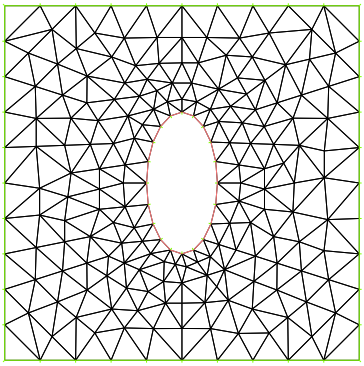

Fig. 4. Square mesh with a hole in FreeFem++.

As we did with our own codes in § 4.1, a convergence analysis of the first mode was also performed for the square domain using FreeFem++. The results for the error of the first natural frequency are presented in Fig. 5 and follow the same trend that we obtained with our code.

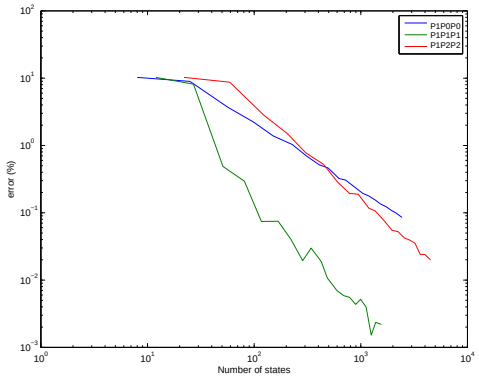

Fig. 5. Convergence of the first natural frequency of the 2D linear wave equation, discretization using FreeFem++.

5. PERSPECTIVES AND CONCLUSIONS

Two extensions of the PFEM are proposed before concluding.

5.1 Extension to other coordinate systems

The method presented above was written in cartesian coordinates. For other geometries, it can be easier to deal with other curvilinear systems, like the polar coordinates. In this latter case, the methodology to obtain the discretized equations remain the same: for example, in (26), the same kind of algebraic structure is obtain for J, with matrices D_ρ and D_θ and their transpose. For the choice of the basis functions, polynomials are suitable for the ρ variable, but care must be taken to use periodic functions for the θ variable: trigonometric polynomials will solve this problem, as detailed in (Boyd, 2001, chap. 18).

5.2 Extension to nonlinear equations

In the previous section, we performed the discretization of a linear wave equation with a quadratic Hamiltonian (29). Nonlinear equations like the shallow water equations (SWE), exhibit the same interconnection structure as (1) with power balance (9). The difference lies in the fact that the Hamiltonian is non-quadratic (and, for this reason, the constitutive equations are nonlinear).

In the case of the 2D irrotational SWE, the Hamiltonian can be written as:

$$H = \frac{1}{2}\int_\Omega \left(\frac{1}{\rho}\alpha_3 \left(\alpha_1^2 + \alpha_2^2\right) + \rho g \alpha_3^2\right) \mathrm{d}\Omega \ . \qquad (33)$$

In the case of non-quadratic Hamiltonian, the derivation of the discretized Hamiltonian is not as straightforward as in the quadratic case (that is, obtaining (30) from (29)). Nevertheless, it is possible to approximate the Hamiltonian using integration by numerical quadrature. Indeed, since the variables are approximated using polynomial basis functions, and since the integrand of the Hamiltonian (33) is also a polynomial, the discretized Hamiltonian can be exactly computed by quadrature.

5.3 Conclusions

This paper presents the PFEM, a new method for the power-preserving discretization of 2D wave equation. Rewriting the wave equation in a weak-form where only some of the equations are integrated by parts, a skew-symmetric representation naturally arises with the boundary control and observation. After discretization, a finite-dimensional port-Hamiltonian system is obtained in a straightforward way.

The PFEM method can be easily implemented using available Finite Element software (for instance, opensource software as FreeFem++ (Hecht, 2012)), since it suffices to properly write the weak-form equations.

An even greater flexibility comes from the choice of the boundary inputs and outputs, either by a conservative change of boundary variables through an orthogonal matrix, or by the choice of the partition of the variables in the process of integration by parts.

The extension of the method to other coordinate systems, and to nonlinear equations will be better explored in further work, (Cardoso-Ribeiro et al., 2018).

REFERENCES

Boyd, J.P. (2001). *Chebyshev and Fourier spectral methods*. Dover.

Cardoso-Ribeiro, F.L., Matignon, D., and Pommier-Budinger, V. (2016). Piezoelectric beam with distributed control ports : a power-preserving discretization using weak formulation. In *2nd IFAC Workshop on Control of Systems Governed by Partial Differential Equations (CPDE)*, 290–297. Bertinoro, Italy.

Cardoso-Ribeiro, F.L., Matignon, D., and Lefèvre, L. (2018). A Partitioned Finite-Element Method for power-preserving discretization of open systems of conservation laws. *Preprint, to be submitted*.

Duindam, V., Macchelli, A., Stramigioli, S., and Bruyninckx, H. (2009). *Modeling and Control of Complex Physical Systems: The Port-Hamiltonian Approach*. Springer Berlin Heidelberg, Berlin, Heidelberg.

Farle, O., Klis, D., Jochum, M., Floch, O., and Dyczij-Edlinger, R. (2013). A port-Hamiltonian finite-element formulation for the Maxwell equations. *Proceedings of the 2013 International Conference on Electromagnetics in Advanced Applications, ICEAA 2013*, (4), 324–327.

Farle, O., Baltes, R.B., and Dyczij-Edlinger, R. (2014a). A Port-Hamiltonian Finite-Element Formulation for the Transmission Line. In *Proceedings of 21st International Symposium on Mathematical Theory of Networks and Systems*, 724–728. Groningen, The Netherlands.

Farle, O., Baltes, R.B., and Dyczij-Edlinger, R. (2014b). Strukturerhaltende Diskretisierung verteilt-parametrischer Port-Hamiltonscher Systeme mittels finiter Elemente. *at - Automatisierungstechnik*, 62(7), 500–511.

Golo, G., Talasila, V., van der Schaft, A.J., and Maschke, B. (2004). Hamiltonian discretization of boundary control systems. *Automatica*, 40(5), 757–771.

Hecht, F. (2012). New development in FreeFem++. *J. Numer. Math.*, 20(3-4), 251–265.

Hiemstra, R., Toshniwal, D., Huijsmans, R., and Gerritsma, M. (2014). High order geometric methods with exact conservation properties. *Journal of Computational Physics*, 257, 1444–1471.

Kotyczka, P. (2016). Finite Volume Structure-Preserving Discretization of Distributed-Parameter Port-Hamiltonian Systems. In *2nd IFAC Workshop on Control of Systems Governed by Partial Differential Equations (CPDE)*, volume 49, 298–303. Elsevier B.V., Bertinoro, Italy.

Kotyczka, P., Maschke, B., and Lefèvre, L. (2018). Weak form of Stokes-Dirac structures and geometric discretization of port-Hamiltonian systems. *Journal of Computational Physics*, 361, 442–476.

Moulla, R., Lefevre, L., and Maschke, B. (2012). Pseudo-spectral methods for the spatial symplectic reduction of open systems of conservation laws. *Journal of Computational Physics*, 231(4), 1272–1292.

Trenchant, V., Ramirez, H., Gorrec, Y.L., and Kotyczka, P. (2017). Structure preserving spatial discretization of 2D hyperbolic systems using staggered grids finite difference. In *Proceedings of the 2017 American Control Conference*. Seattle, USA.

Vu, N.M.T., Lefèvre, L., and Maschke, B. (2016). A structured control model for the thermo-magneto-hydrodynamics of plasmas in tokamaks. *Mathematical and Computer Modelling of Dynamical Systems*, 22(3), 181–206.

Vu, N., Lefèvre, L., Nouailletas, R., and Brémond, S. (2017). Symplectic spatial integration schemes for systems of balance equations. *Journal of Process Control*, 51, 1–17.

Wu, Y., Hamroun, B., Le Gorrec, Y., and Maschke, B. (2015). Power preserving model reduction of 2D vibro-acoustic system: A port Hamiltonian approach. *Proceedings of the 5th IFAC Workshop on Lagrangian and Hamiltonian Methods for Nonlinear Control (LHMNC)*, 48(13), 206–211.